Published in final edited form as:
J Proteome Res. 2012 February 3; 11(2): 1163–1174. doi:10.1021/pr2008972.

Protein composition of immunoprecipitated synaptic ribbons

A. Kantardzhieva[1], **M. Peppi**[1], **W.S. Lane**[2], and **W.F. Sewell**[1,*]

[1]Eaton-Peabody Laboratory, Department of Otology and Laryngology, Massachusetts Eye and Ear Infirmary and Harvard Medical School, 243 Charles Street, Boston, MA 02114

[2]Harvard Mass Spectrometry and Proteomics Resource Lab; FAS Center for Systems Biology, Harvard University, Cambridge, Massachusetts 02138

Abstract

The synaptic ribbon is an electron-dense structure found in hair cells and photoreceptors. The ribbon is surrounded by neurotransmitter-filled vesicles and considered to play a role in vesicle release. We generated an objective, quantitative analysis of the protein composition of the ribbon complex using a mass spectrometry-based proteomics analysis. Our use of affinity-purified ribbons and control IgG immunoprecipitations ensure that the identified proteins are indeed associated with the ribbon complex. The use of mouse tissue, where the proteome is complete, generated a comprehensive analysis of the candidates. We identified 30 proteins (comprising 56 isoforms and subunits) associated with the ribbon complex. The ribbon complex primarily comprises proteins found in conventional synapses, which we categorized into 6 functional groups: vesicle handling (38.5%), scaffold (7.3%), cytoskeletal molecules (20.6%), phosphorylation enzymes (10.6%), molecular chaperones (8.2%), and transmembrane proteins from the presynaptic membrane firmly attached to the ribbon (11.3%). The 3 CtBP isoforms represent the major protein in the ribbon whether calculated by molar amount (30%) or by mass (20%). The relatively high quantity of phosphorylation enzymes suggests a very active and regulated structure. The ribbon appears to comprise a concentrated cluster of proteins dealing with vesicle creation, retention and distribution, and consequent exocytosis.

Keywords

synapse; synaptic ribbon; proteomics; vesicle release; active zone; retina; cochlea

Introduction

The synaptic ribbon is one of the great enigmas of sensory biology. It sits at the core of some of the most remarkable synapses in the body, yet little is known of its molecular structure or function. Surrounded by neurotransmitter-filled vesicles, it is thought to generate a readily releasable pool of vesicles at the synapse [1–3]. The ribbon is found in photoreceptors and in hair cells – cell types specialized for graded synaptic transmission; they are adapted to release measured amounts of neurotransmitter in response to small changes in membrane potential. Most other synapses in the nervous system respond to transient presynaptic voltages in the form of action potentials. This has led to speculation that the synaptic ribbon may exist to provide a transient response capability to a synapse

Corresponding author: William F. Sewell Eaton-Peabody Laboratory, Massachusetts Eye and Ear Infirmary, 243 Charles Street, Boston, MA 02114, phone: 617-573-3156, fax: 617-720-4408, wfs@epl.meei.harvard.edu.

Supporting information
Supporting Information available: This material is available free of charge via the Internet at http://pubs.acs.org.

otherwise optimized for graded responses [4]. This idea is supported by one of the few functional analyses of the ribbon's role in stimulus coding: *Bassoon* knockout mice have fewer synaptic ribbons, and most are detached from the presynaptic membrane region. The primary deficit in the auditory responses of these mice is a loss of rapid onset responses to stimuli. A secondary deficit is a reduction in both spontaneous and evoked discharge rate, suggesting an additional role enabling sustained high rates of exocytosis [5,6].

Despite an abundance of immunohistochemical and other candidate analyses, there is no quantitative or objective data on the protein composition of the ribbon complex. Uthaiah and Hudspeth recently presented an extensive biochemical analysis of isolated synaptic ribbon complexes that combined immunoblotting, immunohistochemistry, and LC-MS (liquid chromatography-mass spectrometry) proteomics to generate a broad array of strong candidates for function at the ribbon complex [7]. We have taken a complementary approach to identifying the proteins in the ribbon complex, which is to affinity-purify very large quantities of ribbon complex from adult mouse retinas to generate an objective assessment of the major proteins in the synaptic ribbon complex by LC-MS/MS. The affinity purification likely yielded both the ribbon and portions of the presynaptic density, but few of the associated vesicles. The project was by necessity completed on retina ribbons because the number of ribbons required for a quantitative mass spectrometry analysis is not achievable from hair cells, but it is reasonable to assume that the ribbon composition will apply to the auditory system as well.

Experimental Procedures

Animals

Mice, of various strains, 3 – 52 weeks of age were used. Animal procedures were approved by the Animal Care Committee of the Massachusetts Eye and Ear Infirmary.

Purification of synaptic ribbon complexes

Mice were anesthetized with pentobarbital (300 mg/Kg). Eyeballs were removed; the retinas scraped off and kept at −80 °C. Frozen bovine retinas were obtained from PelFreeze (Arkansas). A total of 30 bovine retinas or 1000 murine retinas were utilized for a set of immunoprecipitations (IPs). We modified Schmitz et al's [8,9] ribbon purification protocol, avoiding the last steps, namely the 70–20% sucrose step gradient, and the consequent treatment with 2 M NaCl and high pH. For the mouse retinas we also skipped the preceding 30%–50% sucrose gradient step and reduced the Triton buffer incubation to 5 min in order to increase our protein yield. The final pellets of the murine and bovine ribbon isolation were recovered in IP buffer (50mM Tris pH 7.5, 0.5% Triton X100,150 mM NaCl, 10% Glycerol, 1 mM EGTA, 2 mM $MgCl_2$ and 1 mM of PMSF (phenylmethanesulfonylflouride), and sonicated. The protein yield, amounting to 30 mg of murine material and 22.5 mg of bovine material, was adjusted to 3 μg/ul. Most importantly, we introduced an affinity-purification step with anti-CtBP2 monoclonal antibody (Ab), which recognizes both Ribeye and CtBP2. As a control we used mouse immunoglobulin G (IgG).

Immunoprecipitation and gel separation of ribbon-associated proteins for sequencing

Dynabeads® M-450 Tosylactivated (Invitrogen) were coupled to antibodies according to manufacturer's protocol and cross-linked with dimethyl pimelimidate dihydrochloride (Sigma) for 20 min. Partially purified ribbon fractions (described above) were incubated with 500 μl beads coupled to Ribeye/CtBP2 Ab or normal IgG at 4°C for 4.5h followed by washing in IP buffer. Beads were heated at 80°C in Novex® Tris-Glycin SDS sample buffer (Invitrogen) and the released proteins loaded on NuPAGE 10% Bis-Tris Gel 1.0 mm

(Invitrogen) and separated electrophoretically. Samples were stained with the Novex® colloidal blue kit (Invitrogen). The gels were sliced across the horizontal axis of the lanes into 6 pieces each, the sizes of which varied slightly in accordance of the observed amount of protein bands in them.

Protein Identification

After destaining, gel sections were reduced, carboxyamidomethylated, and digested with trypsin *in gel*. To identify proteins specifically present in the ribbon complex, peptides from each sample section were subjected to microcapillary reverse-phase HPLC directly coupled to the nano-electrospray ionization source of a LTQ-Orbitrap Velos hybrid mass spectrometer (LC/MS/MS). The Orbitrap repetitively surveyed an m/z range from 395 to 1600, while data-dependent MS/MS spectra on the ten most abundant ions in each survey scan were acquired in the linear ion trap. MS/MS spectra were acquired with relative collision energy of 30%, 2.5-Da isolation width, and recurring ions dynamically excluded for 60 s. Preliminary evaluation of peptide-spectrum matches (PSMs) was facilitated using SEQUEST with a 30 ppm mass tolerance against the mouse or bovine subset of the Uniprot Knowledgebase. Using a custom version of the Harvard Proteomics Browser Suite (Thermo Scientific, San Jose CA), PSMs were accepted with mass error <3.0 ppm and score thresholds to attain an estimated false discovery rate of ~1% using a reverse decoy database strategy.

Stringent criteria were applied to all proteins in order for them to be considered ribbon constituents: we required that the protein be present in the CtBP2 pull-down material in quantities al least 4 times higher than in the IgG control and be identified by a minimum of four unique peptides in the CtBP2 immunoprecipitate alone. Protein assignments were designed to be most parsimonious: 1) no peptide spectrum was assigned to more than one protein and, 2) when a peptide sequence could be assigned to more than one protein, the assignment was made to the protein that had accumulated the most peptide spectra. For that reason we have grouped together proteins with highly related sequences such as CtBP1 and CtBP2, ERC1 and ERC2 (also called ELKS and CAST), and Bassoon with Piccolo. When performing the calculations we considered the number of potentially shared peptides to estimate the average number of unique peptides per protein. Each peptide is given a value of 1 if it is not potentially shared with other sequence-related protein isoforms and that value is assigned to the only protein it could belong to. If a peptide is potentially shared by more than one protein in a group, the value of 1 is divided by the number of proteins in the group that could potentially give rise to that peptide upon trypsin digest (see Supplementary Table 1). For example if two isoforms in a group share a peptide each isoform is assigned 0.5 unique peptides, and if there are 3 isoforms sharing a common peptide each isoform is given a value of 0.33. Upon establishing the potential commonality and respective values for each peptide, we calculated the total number of unique peptides per protein isoform. As a simple example if two proteins A and B have been assigned 8 and 2 unique peptides respectively by the algorithm, and 4 of the peptides assigned to protein A are theoretically observable in protein B, we recalculate the proteins A and B to have 6 and 4 unique peptides respectively. Highly related proteins like actins and proteins forming functional protein oligomers such as the subunits voltage-dependent calcium channel were left in the final list of top likely specific co-precipitates (even if they had less than 4 unique peptides or low ratios).

Protein Abundance Determination

We have adapted a method described previously for estimation of relative protein abundance [10]. Our sequencing data has provided the number of unique peptides per protein in both IgG and CtBP fractions. To calculate the number of observable unique peptides per protein, protein sequences were digested *in silico* using the Expasy Peptide Mass tool:

(http://ca.expasy.org/tools/peptide-mass.html) taking into account the experimental conditions used: allowing for two missed cleavages, oxidized methionines, treatment with iodoacetamide, and selecting for molecular weight range of the peptides between 750–4000 Da (comparable with the scan range of the mass spectrometer 700–3500).

The PAI (protein abundance index) is defined as:

$$PAI = \frac{N_{obsd}}{N_{obsbl}}$$

where N_{obsd} and N_{obsbl} are the number of unique observed peptides and the number of unique observable peptides per protein, respectively.

The emPAI (exponentially modified protein abundance index) is defined as:

$$emPAI = 10^{PAI} - 1$$

The protein contents in molar fraction percentages are calculated as:

$$\text{Protein content } (mol\%) = \frac{emPAI}{\sum(emPAI)} \times 100$$

where and Σ (*emPAI)* is the sum of *emPAI* values for all the proteins selected by us to be included in the analysis.

Calculation for the number of unique observable peptides selecting for masses ranging 500–3000 or 500–4000 Da gained similar ratios for the proteins in the mix. Generally the same holds true if all theoretical peptides were included.

Western blots: performed as described previously [11].

Antibodies

CtBP2 and KIF3A (BD Transduction Lab cat # 612044 and 611508, respectively), Bassoon (Assays Designs, cat # SAP7F407), Piccolo (Abcam, cat# ab76186), mouse IgG1κ (Sigma Aldrich, cat # M9269), ATP Synthase 5A1 (ProteinTech Group, cat # 14676-1-AP), secondary antibodies (#A11001, A10042 Invitrogen).

Immunolabeling of mouse retinas and purified/immunoprecipitated synaptic ribbons

Murine eyes or post- IP beads were fixed for 10–20 min in 3.7% paraformaldehyde. The eyes were treated with 30% sucrose/PBS overnight and cryosectioned at 8 μm. An overnight incubation with primary antibodies (diluted 1:200) in 10% normal goat serum was followed PBS wash and incubation with secondary antibodies (dilution1:500) for 1.5 h.

Results and Discussion

Affinity pull-down yielded large quantities of highly purified ribbons

We began by repeating the differential- and density-gradient centrifugation protocol developed by Schmitz et al. [8,9] using cow retinas. Because we observed major losses (99%) of the Ribeye protein (an alternative transcription product of *Ctbp2* considered to be a signature protein of the ribbon [9]) we developed an affinity pull-down procedure to reduce

the loss of material and quantity of impurities (Figures 1 and 2). The efficiency of the IP procedure suggested it should be possible to obtain purified ribbons at earlier steps in the purification protocol- fractions 3 or even 2 which left us with about 30-fold more protein compared with the original procedure using the last (sixth) fraction (Figure 1, right panel).

The purification and immunoprecipitation procedure was scaled up to purify a large quantity of ribbons for proteomics analysis (1000 mouse retinas or 30 cow retinas, see Experimental Procedures). Eluates from the control beads contained mostly antibodies; in the non-reducing conditions used in this experiment they appear as bands of 150 kDa. Eluates from the CtBP2/Ribeye immunoprecipitates had a number of bands that did not appear in the control (Figure 3).

Mass spectrometry based proteomics analysis

LC tandem mass spectrometry proteomics analyses were performed on each slice shown in figure 3 for both the mouse and the bovine retina preparations. Because the bovine proteome is incomplete, and due to the unquantified time between the cow's death and retina freezing, the cow data was used only for corroboration. The description that follows is for the mouse ribbon proteome.

We identified over 2,500 peptides attributed to over 206 different proteins. Quantification of the individual protein amounts was accomplished by calculating the exponentially modified protein abundance index [10]. This method is based on a linear relationship between the logarithm of protein abundance and the protein coverage, the latter calculated as the number of observed *vs.* observable unique peptides. The algorithm is useful for estimating the relative ratios of proteins in a complex sample (see calculation details in Experimental Procedures section). The amount of material needed (1000 retinas) to generate the large numbers of unique peptide fragments for quantification made repeated measurements impractical, limiting our ability to assess the statistical significance of the stoichiometric findings. We have chosen to focus only on the most robustly identified proteins, so our false positive rate should be very low, but of course we may have missed many low stoichiometry proteins.

Of the 206 proteins, 30 were also present in similar quantities in the control IgG immunoprecipitates and thus eliminated from further consideration. Another 6 proteins were eliminated because they were less than four-fold higher in the CtBP2/Ribeye *vs.* control immunoprecipitates. Finally, we excluded from our quantitative analysis 102 proteins that were exclusively present in the CtBP2/Ribeye immunoprecipitates but were represented by less than 4 unique peptide sequences. A few exceptions were made to this selection process for quaternary proteins and highly homologous isoforms (see Experimental Procedures). Because we have used such a conservative selection process, we may have excluded from quantification some proteins present in small amounts in the ribbon (listed in Table 3), but chose to emphasize instead the major components for quantification.

We quantified, with emPAI, the remaining 68 proteins, including isoforms, that were represented by more than 4 unique peptides in CtBP2/Ribeye immunoprecipitates and were either absent or represented by at least 4-fold fewer unique peptides in the control Of these 68 proteins, 12 are typically found in the nucleus. This is not surprising, for CtBP2 is a transcriptional co-repressor and despite our efforts to eliminate the nuclear fraction early in the purification, some contamination remained. We eliminated these 12 as likely candidates to be in the ribbon, and have treated them separately (Table 2). Many of the remaining 56 proteins were either subunits of a quaternary structure or represented by closely related isoforms, allowing the dataset to be compressed to describe 30 proteins that were present in high enough amounts to warrant quantification (Table 1).

Proteins in the ribbon complex

Of the 30 proteins quantified within the ribbon complex, 10 comprised nearly 4/5 (78.5%) of the total molar quantity, and thus are considered major constituents. Each major protein constitutes more than 2% of the total molar protein content. These proteins are: CtBP (30%), Actin (5.9%), Tubulin (10.9%), heat shock proteins (HSPA1b, 5, 8 and 9) (8.2%), ERC (ELKS/CAST) (6.2%), ATP Synthase (5.8%), CaM Kinase II (3%), RAPGEF4 (3.2%), PGAM5 (2.8%), and the GABA-A Receptor (2.5%). The ribbon complex (the ribbon core, a portion of the presynaptic membrane, and any other firmly attached proteins) is for the most part comprised of protein groups found in conventional synapses (Figure 4).

Many of the ribbon proteins have well-established roles in **vesicle handling:** CtBP, ERC, Piccolo, Bassoon, Liprin and RIMBP. They also have well-documented interactions with one other [12–16]. CtBP isoforms dominate this category. Because the sequence homology of the B domain of the CtBP isoforms is very high, and because the A domain of Ribeye was not present in the Uniprot library with which we generated the proteomics analysis, we had to infer the relative proportions of the CtBP isoforms. This was feasible because Ribeye has a much higher molecular weight than the other CtBP isoforms, and thus ran in a different position in the gel, which was consequently analyzed in a separate mass spec run. We estimate that the Ribeye comprised between one third and one half of the total molar amount of the CtBP isoforms. Bassoon is known to play a role in tethering the ribbon to the synaptic complex [6]. A number of other known synaptic proteins were identified exclusively in ribbon immunoprecipitates, but with fewer than 4 unique peptides, so they did not meet the criteria for quantification. These include Synapsin (1 and 2), Rabphilin 3a, Synaptogyrin3, Synaptotagmin1, Clathrin Heavy Chain1, SNAP25, β-2-Syntropihin, Syntaxin-Binding Protein1, and Synaptic Vesicle Glycoprotein 2a (see also Table 3). Our purification procedure (specifically a tritonization step and subsequent sonication) probably stripped attached vesicles from the ribbon complex so that vesicle-associated proteins were absent or under-represented in the mix.

We identified several **transmembrane proteins** that are most likely associated with the synaptic membrane contacting the ribbon core. They include Na/K ATPase, GABA A Receptor, the L-TYPE Calcium Channel, and ATP Synthase. The L-Type Calcium Channel can bind Piccolo and RIMBP[17,18]. GABA-A Receptor α and β subunits were present in equimolar quantities with lesser quantities of the γ subunit. The receptor is a pentamer, and it likely comprises 2 α1 subunits, 2 β (β2 and β3) subunits and a γ subunit [19]. ATP Synthase, once thought of as a mitochondrial enzyme is now known to be present in a variety of other locations in cells [20]. It is unlikely that the ATP Synthase in our ribbon immunoprecipitates is from mitochondria. First, we only identified the alpha and beta (soluble) subunits while the mitochondrial ATP Synthase contains as many as 14 subunits both membrane bound and soluble, located at the inner mitochondrial membrane [21,22]. Second, we co-precipitated very few other mitochondrial proteins, further decreasing the possibility of mitochondrial origin for the ATP synthase. We examined the distribution of ATP Synthase, and CaM Kinase II and observed them located proximal to, though not within, the ribbon, while CtBP1 is located within the ribbon core (Figure 5). GABAA receptors have been localized in the bipolar cells in the retina along with Gephryn, its binding partner [23–27]. The bipolar cells contain part of the CtBP2/Ribeye protein content in the retina [28], thus probably accounting for this co-purification. The localization of PGAM5 protein has been found both in the nucleus and mitochondria [29–31], raising the possibility that it may have been pulled down as a nuclear contaminate.

Synapse-specific molecules are held in place and prevented from diffusion by additional protein interactions with **scaffolding molecules**, which eventually link them to the **cytoskeleton**. Scaffolding molecules we observed include Gephyrin, Catenin, GRIP1,

CASK, Spectrin, Band 4.1 Protein, and Band 4.1 Like Proteins. Among the functionally related group of cytoskeletal proteins were Tubulin, Actin, Vimentin, EML5, NEFL, and Myosin10. CASK is known to anchor transmembrane synaptic proteins like Neurexin and Rabphilin. Gephyrin binds GABA receptors and links them to Tubulins [23,24]. Catenins can bind GRIP1 and also link to the cytoskeleton via their interaction with Actin [32–34]. Actin, Band 4.1 Proteins, Spectrins and Vimentin are known to associate directly [35–39] and Vimentin anchors the position of a number of organelles in the cytosol [40]. Perhaps along with the Tubulins it plays a similar role for the ribbon. Vimentin has also been shown to bind to a SNARE protein SNAP23 [41].

The complex interactions, localizations and activities of the proteins are regulated in part by **kinases and phosphatases.** Most synaptic constituents have putative phosphorylation sites, and for many proteins these sites are characterized [42,43]. We found CaM Kinase II, RAPGEF4 (EPAC2), PPP2R1A and PGAM5 representing 10.6% of the protein, suggesting tight regulation of the ribbon function. CaM Kinase II (Ca-dependent phosphorylation enzyme) regulates Liprin [44] and appears to be located within the structure of the synaptic ribbon [7]. We observed 3 isoforms (α, β, and δ) of CaM Kinase II, with equimolar amounts of α and β and twice as much of the δ isoform. EPAC2 is expressed in photoreceptors[45]; it is known to be involved in cAMP mediated vesicle release [46] and is a binding partner of Piccolo [17] and Rim [47]. Piccolo also binds L-TYPE Ca Channels[17] and an Actin-Binding Protein [48] providing a possible link between members in the presynaptic complex. Phosphoglyceraldehyde mutase (PGAM5) has no mutase activity, but instead serves as a serine-threonine phosphorylation enzyme [49]. The proper folding and chaperoning of these proteins require some of the many **chaperones** in the ribbon precipitates: a number of heat shock proteins are listed in Table 1. In the category **"other"** we have put the S-Arrestin, SCRIN1, Glutamine Synthase and TRIM21 proteins. S-Arrestin participates in agonist-mediated desensitization of G-Protein-Coupled Receptors [50]. Glutamine Synthase converts glutamate to glutamine. It was identified in a previous ribbon proteomics analysis [7]. TRIM21 is a cytosolic IgG receptor and part of the intracellular antibody-mediated proteolysis pathway [51]. We suspect it is a contamination/component in the anti-CtBP2 Ab reagent.

Of the 102 proteins that were excluded from the quantitative analysis above, 24 were present exclusively in the CtBP2/Ribeye immunoprecipitates and had at least 2 unique peptide fragments. These are listed in Table 3, and include a number of proteins known to be associated with synaptic vesicles, including Clathrin, NSF, Rabphilin, Synapsin, Synaptogyrin, and Synaptotagmin.

The synaptic ribbon complex, which consists of the ribbon core and portions of the presynaptic density is primarily composed of proteins associated with vesicle release at the cytomatrix active zone of conventional synapses, suggesting that the molecular mechanisms of vesicle handling and release here may be fundamentally conventional. We have quantified the relative amounts of many proteins that were previously identified in the ribbon through smaller scale proteomics analysis or through candidate analyses (i.e. immunohistochemistry or immunoblotting) [6–8,14], including CtBP isoforms, ERC 1 and 2 (i.e. CAST and ELKS), Bassoon, and Piccolo, CaM Kinase II, Spectrin, Vimentin, Tubulin, NA/K ATPase. Uthaiah and Hudspeth recently investigated the composition of presynaptic proteins isolated by differential and density-gradient centrifugation and affinity-purified CtBP2-containing complexes [7]. The set of proteins isolated with anti-CtBP2 antibodies is partially overlapping with ours. In their work involving CtBP2/Ribeye pull-down they used chicken cochlea material to precipitate with mouse CtBP2 (or Ribeye B-domain) antibody and bovine retina to which they applied rabbit polyclonal Ab raised against the chicken Ribeye's A domain. We view the study as a complementary to ours in which we used

murine or bovine retinal material to precipitate with mouse anti CtBP2 (or Ribeye B-domain) monoclonal Ab. In addition our use of IgG as a control/nonreactive antibody allowed us to eliminate some proteins as not being necessarily associated with the ribbon. Our protocols also varied from those of Uthaiah and Hudspeth in our use of a relatively harsh sonication step, which we suspect may have broken filamentous structures linking the vesicles to the ribbon. As a result of that or simply low interaction strength with the ribbon many exocytosis proteins outlined in their paper were not identified in our analysis, suggesting they may be present in minor quantities or are primarily associated with vesicles.

Our analysis provides a quantitative assessment of the molecular composition of the synaptic ribbon complex based on an exponentially modified protein abundance index [10]. More precise measurements of the absolute amount of particular proteins in the mix are possible, but require knowing the sample's components of interest and the use of high-cost corresponding isotope-labeled peptides as internal standards in methods such as AQUA or QconCAT. We have specified amounts of proteins as molar ratios. Mass ratios for these proteins will differ depending on the molecular weight, and this becomes very different for proteins at the extremes of the spectrum. For this particular mix of proteins, a 71 kDa molecule will have equal molar and mass ratios. Bassoon and Piccolo, at 500 kDa were present collectively in a relatively small molar quantity (1.45%), but high mass ratio (10.5%) while PGAM5, with a molecular weight of 32 kDa, had a high molar ratio (2.82%) but a low mass ratio (1.2%).

The CtBP isoforms, CtBP2 (short), CtBP2 (Ribeye) and CtBP1 together constituted 30% of the total protein content on a molar basis, though our quantities may be exaggerated by the fact that these proteins are primary targets for the pull-down. Given that CtBP is primarily in the ribbon itself and not concentrated in the presynaptic density [6–8,52] it is likely that CtBP isoforms comprise an even greater percentage of the protein in the ribbon itself, corroborating Zenisek's deduction that it could be as high as 2/3 of the protein in the ribbon proper [53]. Quantification of the amounts of the CtBP isoforms in the ribbon is made difficult by their presence in the nucleus. While we know that Ribeye and CtBP1 are localized in the ribbon (Figure 5 and [7]) it hard to confirm/exclude the presence of CtBP2 with immunohistochemistry, for CtBP2 is essentially the B-domain of Ribeye. However judged from our sequencing results where CtBP2 and Ribeye are separated by size in two different gel slices but give rise to shared B-domain peptides, we conclude that the amount of CtBP2 is as much as 1/3 of CtBP isoforms and about equal to Ribeye. Our purification procedure begins with cell lysis followed by nuclear fraction separation by differential centrifugation. Judged from the number of nuclear proteins co-purified with the ribbon, we think some of CtBP2 is of nuclear origin, but the relatively large quantities of CtBP2 we collected implies that CtBP2 in the ribbon as well.

The quantitative analysis of relative molar amounts of protein in the ribbon complex allows us to begin to contemplate the contributions of the major proteins to function. The high molar ratios of CtBP and ERC isoforms indicate prominent roles in ribbon function. CtBP protein family members play a critical role in membrane fission at several intracellular transport steps, including transfer from the Golgi to the epithelial basolateral membrane, fluid-phase endocytosis, macropinocytosis, and retrograde transport of receptors to the endoplasmic reticulum [54–56]. Polymorphic tubular membrane enclosures operate between Golgi complex and the basolateral plasma membrane in epithelial cells. They protrude out of the Golgi complex along microtubules and then detach and migrate to the plasma membrane [57]. When CtBP1 is inactivated (by dominant-negative mutants, blocking Abs or siRNA), these protruding tubules are unable to pinch off the Golgi complex [54]. When Golgi transport is blocked by dominant-negative CtBP1 mutant, the necks of the buds accumulate the mutant protein [58]. Injection of active recombinant CtBP1 leads to rapid formation of

Golgi vesicles almost bypassing the formation of tubular intermediates. The intimate involvement of CtBP1 in vesicle fission in the Golgi suggests that CtBP1 may be acting similarly in the ribbon (see below).

ERC proteins are key to vesicle fusion in other vesicle release systems such as the pancreas [12]. ERC1 binds Bassoon, Piccolo and Rim2 [12] ERC1 is involved in intracellular membrane trafficking [59,60] and is important for the insulin secretion in the pancreatic B cells. It is located in the docking site of the insulin granules and the fusion events of the granules occurs mostly on ERC1 enriched membrane clusters. Overexpression of ERC1 increases exocytosis while knockdown of ERC1 decreases it [61]. Some of our knowledge of ERC proteins also comes from analogous structures and proteins in invertebrates. The neuromuscular junction in *Drosophila* possesses a structure called T-bar, which appears to be an analog of the ribbon [62]. It is known to contain an ERC2 homolog called Bruchpilot, large deletions in which lead to the disintegration of the T-bar [62–65]. With smaller deletions the T-bar has normal size but is devoid of filament-tethered vesicles [66]. These analogies become all the more significant considering that ERC proteins constitute over 6% of the ribbon. A functional link between vesicular proteins and the cytoskeleton can be found in the recently described filaments linking vesicles into discrete clusters at the presynaptic zone of brain neurons. The molecular composition of these filaments is still being investigated. ERC2 immunoreactivity, as well as that of Bassoon is associated with the filaments adjacent to the membrane [67,68]. Bassoon, Piccolo, ERC and Bruchpilot proteins contain contiguous coiled-coil sequences [63,69–71] reminiscent of tethering factors in Golgi and endoplasmic reticulum [72] The coils typically form rod-like structures, believed to establish contacts between membranes at a distance, thereby increasing the specificity or efficiency of the initial attachment/tethering of vesicles [72]. The presence of high proportion of Tubulins and Actins (together contributing close to 17%) suggests a role in vesicle movement, though we do not know how closely they are associated with the ribbon itself.

Our finding of a significant quantity of enzymes (both phosphorylation and metabolic) and chaperone (heat shock) proteins indicates dynamic control of the ribbon. CaM Kinase II performs calcium-dependent phosphorylation to alter protein function while PGAM5 is a serine/threonine phosphatase that dephosphorylates proteins. Phosphorylation enzymes might regulate the availability of vesicles based on changes in intracellular calcium. Because the ribbon is intimately associated with calcium channels that control vesicle release, it is reasonable to suggest that CaM Kinase is activated under conditions that evoke vesicle release or depletion, and then perhaps plays a role in refilling the vesicle docking sites on the ribbon.

Conclusions

Based on our findings of the ribbon composition and known functions of ribbon complex proteins in other systems, we suggest that the synaptic ribbon may function to create, organize, release, and perhaps standardize the size of vesicles at the synaptic ribbon. CtBP may initiate vesicle fission to create vesicles near the ribbon from tubulo-vesicular structures endocytosed around the ribbon. In *Bassoon* knockout mice [6], the ribbon detaches from the synapse, leaving endocytic membrane retrieval normal, but an accumulation of tubular and cisternal membrane structures occurs at the presynaptic densities. Many membranous structures are also accumulated around the floating ribbons and they have vesicle-like appearance when located very close to the ribbon, and cisternal appearance when located away from the ribbon. These membrane structures are similar to those observed at synapses following strong stimulation [73,74]. So perhaps CtBP proteins, via fission, parse these endocytic structures into new synaptic vesicles, which then remain associated with the ribbon and repopulate the readily-releasable pool. Additional support for this hypothesis

comes from electron tomography on frog hair cells to recreate the fine structure the ribbon synapses [74]. Prolonged maximal excitation of the synapse depleted 70% of the vesicles in its close vicinity, and led to the appearance of intracellular cisterns and membrane invaginations accounting for the most part of vesicular membrane loss. The authors conclude that formation of new synaptic vesicles from the observed cisterns and membrane invaginations is the rate-limiting step in the vesicle recycling, suggesting that even when functioning normally, the ribbon may not always be able to keep up with abnormally high rates of transmitter release and endocytosis.

Once vesicles are created, vesicle-handling proteins such as the ERC1 and ERC2, Bassoon, and Piccolo may organize them around the ribbon. Cytoskeletal proteins like Actin and Tubulin may organize the structure or participate in moving the vesicles about the surface of the ribbon. The presence of a large quantity of phosphorylation proteins may indicate a relatively active process, changing it performance characteristics with varying demand. In summary, proteomics analysis of the ribbon complex suggests this structure is a highly organized and concentrated cluster of proteins dealing with vesicle creation, retention and distribution and consequent exocytosis (this idea is illustrated in Figure 6). The relatively high quantities of CTBP and ERC isoforms suggest a significant role for those proteins in the ribbon function. Given observations in other systems that these proteins play roles in vesicle fission and handling, we hypothesize a similar function for these proteins in the synaptic ribbon.

Supplementary Material

Refer to Web version on PubMed Central for supplementary material.

Acknowledgments

The work was supported by the NIDCD (DC767 and DC9651). We appreciate the contributions of J. Evans of the U. Mass proteomics facility. We thank R. A. Eatock, M. C. Brown, and M. C. Liberman for comments on earlier versions of the manuscript.

References

1. Glowatzki E, Grant L, Fuchs P. Hair cell afferent synapses. Current opinion in neurobiology. 2008; 18:389–95. [PubMed: 18824101]
2. Moser T, Brandt A, Lysakowski A. Hair cell ribbon synapses. Cell and tissue research. 2006; 326:347–59. [PubMed: 16944206]
3. Sterling P, Matthews G. Structure and function of ribbon synapses. Trends in neurosciences. 2005; 28:20–9. [PubMed: 15626493]
4. LoGiudice L, Matthews G. The role of ribbons at sensory synapses. Neuroscientist. 2009; 15:380–91. [PubMed: 19264728]
5. Buran BN, Strenzke N, Neef A, Gundelfinger ED, Moser T, Liberman MC. Onset coding is degraded in auditory nerve fibers from mutant mice lacking synaptic ribbons. J Neurosci. 2010; 30:7587–97. [PubMed: 20519533]
6. Khimich D, Nouvian R, Pujol R, Tom Dieck S, Egner A, Gundelfinger ED, Moser T. Hair cell synaptic ribbons are essential for synchronous auditory signalling. Nature. 2005; 434:889–94. [PubMed: 15829963]
7. Uthaiah RC, Hudspeth AJ. Molecular anatomy of the hair cell's ribbon synapse. J Neurosci. 2010; 30:12387–99. [PubMed: 20844134]
8. Schmitz F, Bechmann M, Drenckhahn D. Purification of synaptic ribbons, structural components of the photoreceptor active zone complex. J Neurosci. 1996; 16:7109–16. [PubMed: 8929420]

9. Schmitz F, Konigstorfer A, Sudhof TC. RIBEYE, a component of synaptic ribbons: a protein's journey through evolution provides insight into synaptic ribbon function. Neuron. 2000; 28:857–72. [PubMed: 11163272]
10. Ishihama Y, Oda Y, Tabata T, Sato T, Nagasu T, Rappsilber J, Mann M. Exponentially modified protein abundance index (emPAI) for estimation of absolute protein amount in proteomics by the number of sequenced peptides per protein. Mol Cell Proteomics. 2005; 4:1265–72. [PubMed: 15958392]
11. Kantardzhieva A, Alexeeva S, Versteeg I, Wijnholds J. MPP3 is recruited to the MPP5 protein scaffold at the retinal outer limiting membrane. FEBS J. 2006; 273:1152–65. [PubMed: 16519681]
12. Ohara-Imaizumi M, Ohtsuka T, Matsushima S, Akimoto Y, Nishiwaki C, Nakamichi Y, Kikuta T, Nagai S, Kawakami H, Watanabe T, Nagamatsu S. ELKS, a protein structurally related to the active zone-associated protein CAST, is expressed in pancreatic beta cells and functions in insulin exocytosis: interaction of ELKS with exocytotic machinery analyzed by total internal reflection fluorescence microscopy. Mol Biol Cell. 2005; 16:3289–300. [PubMed: 15888548]
13. tom Dieck S, Altrock WD, Kessels MM, Qualmann B, Regus H, Brauner D, Fejtova A, Bracko O, Gundelfinger ED, Brandstatter JH. Molecular dissection of the photoreceptor ribbon synapse: physical interaction of Bassoon and RIBEYE is essential for the assembly of the ribbon complex. J Cell Biol. 2005; 168:825–36. [PubMed: 15728193]
14. Deguchi-Tawarada M, Inoue E, Takao-Rikitsu E, Inoue M, Ohtsuka T, Takai Y. CAST2: identification and characterization of a protein structurally related to the presynaptic cytomatrix protein CAST. Genes Cells. 2004; 9:15–23. [PubMed: 14723704]
15. Takao-Rikitsu E, Mochida S, Inoue E, Deguchi-Tawarada M, Inoue M, Ohtsuka T, Takai Y. Physical and functional interaction of the active zone proteins, CAST, RIM1, and Bassoon, in neurotransmitter release. J Cell Biol. 2004; 164:301–11. [PubMed: 14734538]
16. Ko J, Na M, Kim S, Lee JR, Kim E. Interaction of the ERC family of RIM-binding proteins with the liprin-alpha family of multidomain proteins. J Biol Chem. 2003; 278:42377–85. [PubMed: 12923177]
17. Shibasaki T, Sunaga Y, Fujimoto K, Kashima Y, Seino S. Interaction of ATP sensor, cAMP sensor, Ca2+ sensor, and voltage-dependent Ca2+ channel in insulin granule exocytosis. J Biol Chem. 2004; 279:7956–61. [PubMed: 14660679]
18. Hibino H, Pironkova R, Onwumere O, Vologodskaia M, Hudspeth AJ, Lesage F. RIM binding proteins (RBPs) couple Rab3-interacting molecules (RIMs) to voltage-gated Ca(2+) channels. Neuron. 2002; 34:411–23. [PubMed: 11988172]
19. Sigel E, Baur R, Boulineau N, Minier F. Impact of subunit positioning on GABAA receptor function. Biochem Soc Trans. 2006; 34:868–71. [PubMed: 17052217]
20. Hong S, Pedersen PL. ATP synthase and the actions of inhibitors utilized to study its roles in human health, disease, and other scientific areas. Microbiol Mol Biol Rev. 2008; 72:590–641. Table of Contents. [PubMed: 19052322]
21. Abrahams JP, Leslie AG, Lutter R, Walker JE. Structure at 2. 8 A resolution of F1-ATPase from bovine heart mitochondria. Nature. 1994; 370:621–8. [PubMed: 8065448]
22. Collinson IR, Runswick MJ, Buchanan SK, Fearnley IM, Skehel JM, van Raaij MJ, Griffiths DE, Walker JE. Fo membrane domain of ATP synthase from bovine heart mitochondria: purification, subunit composition, and reconstitution with F1-ATPase. Biochemistry. 1994; 33:7971–8. [PubMed: 8011660]
23. Saiepour L, Fuchs C, Patrizi A, Sassoe-Pognetto M, Harvey RJ, Harvey K. Complex role of collybistin and gephyrin in GABAA receptor clustering. J Biol Chem. 2010; 285:29623–31. [PubMed: 20622020]
24. Prior P, Schmitt B, Grenningloh G, Pribilla I, Multhaup G, Beyreuther K, Maulet Y, Werner P, Langosch D, Kirsch J, et al. Primary structure and alternative splice variants of gephyrin, a putative glycine receptor-tubulin linker protein. Neuron. 1992; 8:1161–70. [PubMed: 1319186]
25. Sassoe-Pognetto M, Kirsch J, Grunert U, Greferath U, Fritschy JM, Mohler H, Betz H, Wassle H. Colocalization of gephyrin and GABAA-receptor subunits in the rat retina. J Comp Neurol. 1995; 357:1–14. [PubMed: 7673460]

26. Greferath U, Grunert U, Fritschy JM, Stephenson A, Mohler H, Wassle H. GABAA receptor subunits have differential distributions in the rat retina: in situ hybridization and immunohistochemistry. J Comp Neurol. 1995; 353:553–71. [PubMed: 7759615]
27. Yue L, Xie A, Bruzik KS, Frolund B, Qian H, Pepperberg DR. Potentiating action of propofol at GABAA receptors of retinal bipolar cells. Invest Ophthalmol Vis Sci. 2011; 52:2497–509. [PubMed: 21071744]
28. Ostergaard J, Hannibal J, Fahrenkrug J. Synaptic contact between melanopsin-containing retinal ganglion cells and rod bipolar cells. Invest Ophthalmol Vis Sci. 2007; 48:3812–20. [PubMed: 17652756]
29. Lo SC, Hannink M. PGAM5, a Bcl-XL-interacting protein, is a novel substrate for the redox-regulated Keap1-dependent ubiquitin ligase complex. J Biol Chem. 2006; 281:37893–903. [PubMed: 17046835]
30. Lo SC, Hannink M. PGAM5 tethers a ternary complex containing Keap1 and Nrf2 to mitochondria. Exp Cell Res. 2008; 314:1789–803. [PubMed: 18387606]
31. Imai Y, Kanao T, Sawada T, Kobayashi Y, Moriwaki Y, Ishida Y, Takeda K, Ichijo H, Lu B, Takahashi R. The loss of PGAM5 suppresses the mitochondrial degeneration caused by inactivation of PINK1 in Drosophila. PLoS Genet. 2010; 6:e1001229. [PubMed: 21151955]
32. Li H, Kim JH, Koh SS, Stallcup MR. Synergistic effects of coactivators GRIP1 and beta-catenin on gene activation: cross-talk between androgen receptor and Wnt signaling pathways. J Biol Chem. 2004; 279:4212–20. [PubMed: 14638683]
33. Rimm DL, Koslov ER, Kebriaei P, Cianci CD, Morrow JS. Alpha 1(E)-catenin is an actin-binding and -bundling protein mediating the attachment of F-actin to the membrane adhesion complex. Proc Natl Acad Sci U S A. 1995; 92:8813–7. [PubMed: 7568023]
34. Ozawa M, Ringwald M, Kemler R. Uvomorulin-catenin complex formation is regulated by a specific domain in the cytoplasmic region of the cell adhesion molecule. Proc Natl Acad Sci U S A. 1990; 87:4246–50. [PubMed: 2349235]
35. Gerke V, Weber K. Identity of p36K phosphorylated upon Rous sarcoma virus transformation with a protein purified from brush borders; calcium-dependent binding to non-erythroid spectrin and F-actin. EMBO J. 1984; 3:227–33. [PubMed: 6323166]
36. Burridge K, Kelly T, Mangeat P. Nonerythrocyte spectrins: actin-membrane attachment proteins occurring in many cell types. J Cell Biol. 1982; 95:478–86. [PubMed: 6183274]
37. Takeshita K, MacDonald RI, MacDonald RC. Band 4. 1 enhances spectrin binding to phosphatidylserine vesicles. Biochem Biophys Res Commun. 1993; 191:165–71. [PubMed: 8447820]
38. Tyler JM, Hargreaves WR, Branton D. Purification of two spectrin-binding proteins: biochemical and electron microscopic evidence for site-specific reassociation between spectrin and bands 2.1 and 4. 1. Proc Natl Acad Sci U S A. 1979; 76:5192–6. [PubMed: 291934]
39. Correia I, Chu D, Chou YH, Goldman RD, Matsudaira P. Integrating the actin and vimentin cytoskeletons. adhesion-dependent formation of fimbrin-vimentin complexes in macrophages. J Cell Biol. 1999; 146:831–42. [PubMed: 10459017]
40. Katsumoto T, Mitsushima A, Kurimura T. The role of the vimentin intermediate filaments in rat 3Y1 cells elucidated by immunoelectron microscopy and computer-graphic reconstruction. Biol Cell. 1990; 68:139–46. [PubMed: 2192768]
41. Faigle W, Colucci-Guyon E, Louvard D, Amigorena S, Galli T. Vimentin filaments in fibroblasts are a reservoir for SNAP23: a component of the membrane fusion machinery. Mol Biol Cell. 2000; 11:3485–94. [PubMed: 11029050]
42. Lonart G, Schoch S, Kaeser PS, Larkin CJ, Sudhof TC, Linden DJ. Phosphorylation of RIM1alpha by PKA triggers presynaptic long-term potentiation at cerebellar parallel fiber synapses. Cell. 2003; 115:49–60. [PubMed: 14532002]
43. Greengard P, Valtorta F, Czernik AJ, Benfenati F. Synaptic vesicle phosphoproteins and regulation of synaptic function. Science. 1993; 259:780–5. [PubMed: 8430330]
44. Hoogenraad CC, Feliu-Mojer MI, Spangler SA, Milstein AD, Dunah AW, Hung AY, Sheng M. Liprinalpha1 degradation by calcium/calmodulin-dependent protein kinase II regulates LAR

receptor tyrosine phosphatase distribution and dendrite development. Dev Cell. 2007; 12:587–602. [PubMed: 17419996]

45. Whitaker CM, Cooper NG. Differential distribution of exchange proteins directly activated by cyclic AMP within the adult rat retina. Neuroscience. 2010; 165:955–67. [PubMed: 19883736]
46. Sedej S, Rose T, Rupnik M. cAMP increases Ca2+-dependent exocytosis through both PKA and Epac2 in mouse melanotrophs from pituitary tissue slices. J Physiol. 2005; 567:799–813. [PubMed: 15994184]
47. Ozaki N, Shibasaki T, Kashima Y, Miki T, Takahashi K, Ueno H, Sunaga Y, Yano H, Matsuura Y, Iwanaga T, Takai Y, Seino S. cAMP-GEFII is a direct target of cAMP in regulated exocytosis. Nat Cell Biol. 2000; 2:805–11. [PubMed: 11056535]
48. Fenster SD, Kessels MM, Qualmann B, Chung WJ, Nash J, Gundelfinger ED, Garner CC. Interactions between Piccolo and the actin/dynamin-binding protein Abp1 link vesicle endocytosis to presynaptic active zones. J Biol Chem. 2003; 278:20268–77. [PubMed: 12654920]
49. Takeda K, Komuro Y, Hayakawa T, Oguchi H, Ishida Y, Murakami S, Noguchi T, Kinoshita H, Sekine Y, Iemura S, Natsume T, Ichijo H. Mitochondrial phosphoglycerate mutase 5 uses alternate catalytic activity as a protein serine/threonine phosphatase to activate ASK1. Proc Natl Acad Sci U S A. 2009; 106:12301–5. [PubMed: 19590015]
50. Palczewski K, McDowell JH, Jakes S, Ingebritsen TS, Hargrave PA. Regulation of rhodopsin dephosphorylation by arrestin. J Biol Chem. 1989; 264:15770–3. [PubMed: 2550422]
51. Mallery DL, McEwan WA, Bidgood SR, Towers GJ, Johnson CM, James LC. Antibodies mediate intracellular immunity through tripartite motif-containing 21 (TRIM21). Proc Natl Acad Sci U S A. 2010; 107:19985–90. [PubMed: 21045130]
52. Dick O, tom Dieck S, Altrock WD, Ammermuller J, Weiler R, Garner CC, Gundelfinger ED, Brandstatter JH. The presynaptic active zone protein bassoon is essential for photoreceptor ribbon synapse formation in the retina. Neuron. 2003; 37:775–86. [PubMed: 12628168]
53. Zenisek D, Horst NK, Merrifield C, Sterling P, Matthews G. Visualizing synaptic ribbons in the living cell. J Neurosci. 2004; 24:9752–9. [PubMed: 15525760]
54. Bonazzi M, Spano S, Turacchio G, Cericola C, Valente C, Colanzi A, Kweon HS, Hsu VW, Polishchuck EV, Polishchuck RS, Sallese M, Pulvirenti T, Corda D, Luini A. CtBP3/BARS drives membrane fission in dynamin-independent transport pathways. Nat Cell Biol. 2005; 7:570–80. [PubMed: 15880102]
55. Corda D, Colanzi A, Luini A. The multiple activities of CtBP/BARS proteins: the Golgi view. Trends Cell Biol. 2006; 16:167–73. [PubMed: 16483777]
56. Haga Y, Miwa N, Jahangeer S, Okada T, Nakamura S. CtBP1/BARS is an activator of phospholipase D1 necessary for agonist-induced macropinocytosis. EMBO J. 2009; 28:1197–207. [PubMed: 19322195]
57. Polishchuk EV, Di Pentima A, Luini A, Polishchuk RS. Mechanism of constitutive export from the golgi: bulk flow via the formation, protrusion, and en bloc cleavage of large trans-golgi network tubular domains. Mol Biol Cell. 2003; 14:4470–85. [PubMed: 12937271]
58. Yang JS, Lee SY, Spano S, Gad H, Zhang L, Nie Z, Bonazzi M, Corda D, Luini A, Hsu VW. A role for BARS at the fission step of COPI vesicle formation from Golgi membrane. EMBO J. 2005; 24:4133–43. [PubMed: 16292346]
59. Monier S, Jollivet F, Janoueix-Lerosey I, Johannes L, Goud B. Characterization of novel Rab6-interacting proteins involved in endosome-to-TGN transport. Traffic. 2002; 3:289–97. [PubMed: 11929610]
60. Wang Y, Liu X, Biederer T, Sudhof TC. A family of RIM-binding proteins regulated by alternative splicing: Implications for the genesis of synaptic active zones. Proc Natl Acad Sci U S A. 2002; 99:14464–9. [PubMed: 12391317]
61. Nomura H, Ohtsuka T, Tadokoro S, Tanaka M, Hirashima N. Involvement of ELKS, an active zone protein, in exocytotic release from RBL-2H3 cells. Cell Immunol. 2009; 258:204–11. [PubMed: 19515363]
62. Fouquet W, Owald D, Wichmann C, Mertel S, Depner H, Dyba M, Hallermann S, Kittel RJ, Eimer S, Sigrist SJ. Maturation of active zone assembly by Drosophila Bruchpilot. J Cell Biol. 2009; 186:129–45. [PubMed: 19596851]

63. Wagh DA, Rasse TM, Asan E, Hofbauer A, Schwenkert I, Durrbeck H, Buchner S, Dabauvalle MC, Schmidt M, Qin G, Wichmann C, Kittel R, Sigrist SJ, Buchner E. Bruchpilot, a protein with homology to ELKS/CAST, is required for structural integrity and function of synaptic active zones in Drosophila. Neuron. 2006; 49:833–44. [PubMed: 16543132]
64. Kittel RJ, Wichmann C, Rasse TM, Fouquet W, Schmidt M, Schmid A, Wagh DA, Pawlu C, Kellner RR, Willig KI, Hell SW, Buchner E, Heckmann M, Sigrist SJ. Bruchpilot promotes active zone assembly, Ca2+ channel clustering, and vesicle release. Science. 2006; 312:1051–4. [PubMed: 16614170]
65. Allport JR, Donnelly LE, Kefalas P, Lo G, Nunn A, Yadollahi-Farsani M, Rendell NB, Murray S, Taylor GW, MacDermot J. A possible role for mono (ADP-ribosyl) transferase in the signalling pathway mediating neutrophil chemotaxis. Br J Clin Pharmacol. 1996; 42:99–106. [PubMed: 8807150]
66. Hallermann S, Kittel RJ, Wichmann C, Weyhersmuller A, Fouquet W, Mertel S, Owald D, Eimer S, Depner H, Schwarzel M, Sigrist SJ, Heckmann M. Naked dense bodies provoke depression. J Neurosci. 2010; 30:14340–5. [PubMed: 20980589]
67. Siksou L, Rostaing P, Lechaire JP, Boudier T, Ohtsuka T, Fejtova A, Kao HT, Greengard P, Gundelfinger ED, Triller A, Marty S. Three-dimensional architecture of presynaptic terminal cytomatrix. J Neurosci. 2007; 27:6868–77. [PubMed: 17596435]
68. Fernandez-Busnadiego R, Zuber B, Maurer UE, Cyrklaff M, Baumeister W, Lucic V. Quantitative analysis of the native presynaptic cytomatrix by cryoelectron tomography. J Cell Biol. 2010; 188:145–56. [PubMed: 20065095]
69. Lupashin V, Sztul E. Golgi tethering factors. Biochim Biophys Acta. 2005; 1744:325–39. [PubMed: 15979505]
70. Wang X, Hu B, Zieba A, Neumann NG, Kasper-Sonnenberg M, Honsbein A, Hultqvist G, Conze T, Witt W, Limbach C, Geitmann M, Danielson H, Kolarow R, Niemann G, Lessmann V, Kilimann MW. A protein interaction node at the neurotransmitter release site: domains of Aczonin/Piccolo, Bassoon, CAST, and rim converge on the N-terminal domain of Munc13-1. J Neurosci. 2009; 29:12584–96. [PubMed: 19812333]
71. Fenster SD, Chung WJ, Zhai R, Cases-Langhoff C, Voss B, Garner AM, Kaempf U, Kindler S, Gundelfinger ED, Garner CC. Piccolo, a presynaptic zinc finger protein structurally related to bassoon. Neuron. 2000; 25:203–14. [PubMed: 10707984]
72. Guo W, Sacher M, Barrowman J, Ferro-Novick S, Novick P. Protein complexes in transport vesicle targeting. Trends Cell Biol. 2000; 10:251–5. [PubMed: 10802541]
73. Holt M, Cooke A, Wu MM, Lagnado L. Bulk membrane retrieval in the synaptic terminal of retinal bipolar cells. J Neurosci. 2003; 23:1329–39. [PubMed: 12598621]
74. Lenzi D, Crum J, Ellisman MH, Roberts WM. Depolarization redistributes synaptic membrane and creates a gradient of vesicles on the synaptic body at a ribbon synapse. Neuron. 2002; 36:649–59. [PubMed: 12441054]

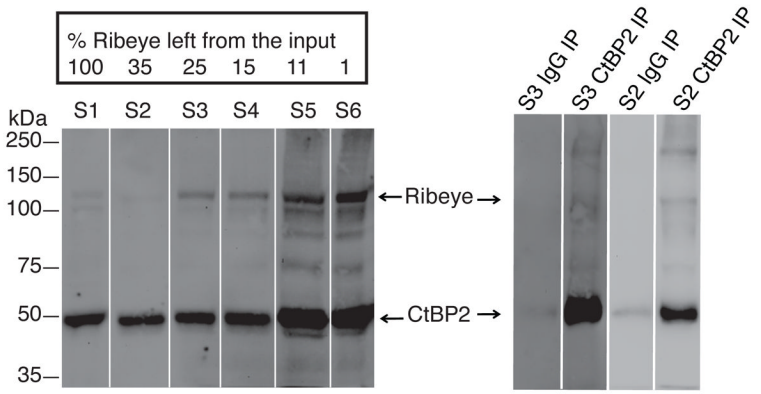

Figure 1.

Left panel: Loss of Ribeye during the purification scheme used for ribbon isolation based on the protocol developed originally by Schmitz. Western blots were used to separate Ribeye from CtBP2 (short) allowing calculation of the ramaining amount of Ribeye, based on sample volume, intensity of Ribeye's Western blot signal, and percent loaded material for each sample. CtBP2 Ab detects both CtBP2 and Ribeye running at 50 and 120 kDa respectively. With each additional purification step, the Ribeye signal became more pronounced relative to the CtBP2 isoform.

Right panel: Immunoprecipitation with CtBP2/Ribeye or control IgG antibody on fractions 3 (S3) and 2 (S2) from the ribbon purification. The control IgG Ab has little background binding of CtBP2. The CtBP2 pull-down lanes have a very strong band around 50 kDa corresponding to the CtBP2 (short) isoform and a weakly stained, longer form running at 120 kDa and corresponding to the Ribeye isoform. The high molecular weight band above might represent multimers of the CtBP2 isoforms for it appears specifically in the CtBP2/Ribeye IP lanes only.

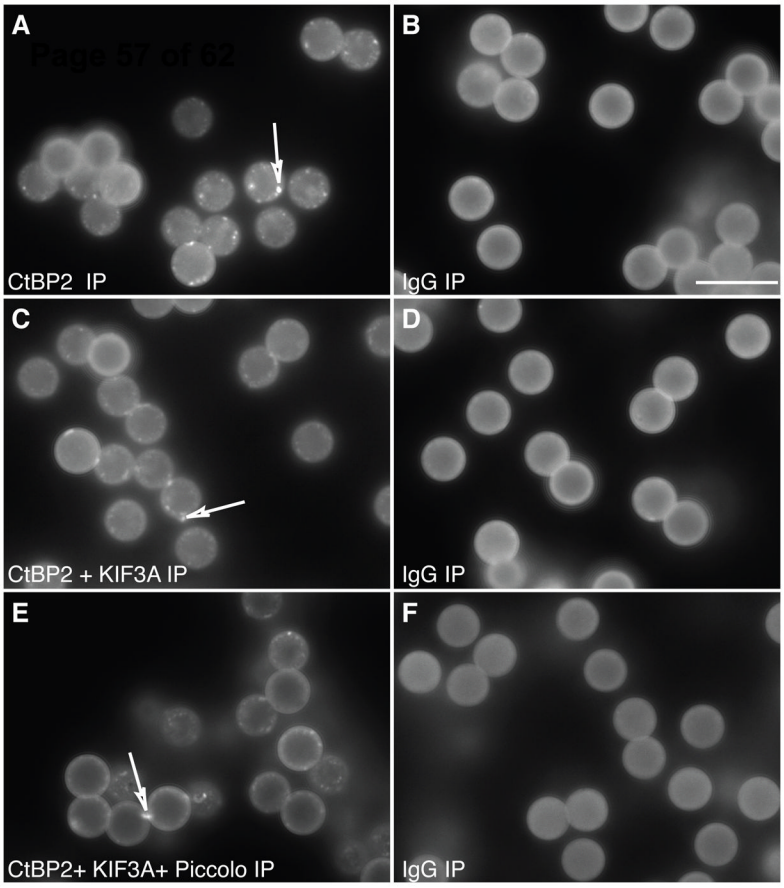

Figure 2. Affinity purified ribbons attached to magnetic beads

Antibodies for proteins known to be in the ribbon were coupled to magnetic beads. The results were optimized by visualizing the precipitated ribbons with immunolabeling for CtBP2/Ribeye. Ribbons could be pulled down with antibodies for CtBP2 (corresponding to the B domain of Ribeye isoform), KIF3A, and Piccolo. The quantity of ribbons pulled down with CtBP2/Ribeye was not increased by adding antibodies to other ribbon proteins such as Piccolo and/or KIF3A (A, C, E). As a control for nonspecific binding, we used mouse IgG (B, D and F). The beads exhibit a degree of autofluorescence. The bright dots (indicated by arrows) in A, C, and E are partially broken ribbons. Due to the spherical structure of the beads, only the periphery is in focus at these pictures. In reality the entire bead is covered with ribbons. Scale bar (in B) 10 μm.

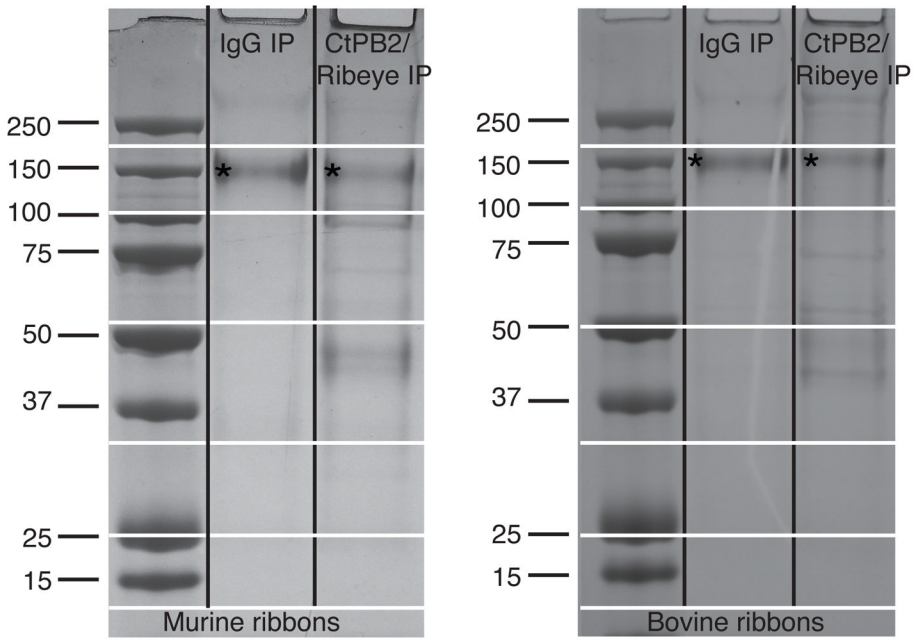

Figure 3. Coomassie Blue staining of the affinity purified ribbons using CtBP2 antibody and control IgG

The 150 kDa non-reduced Ab molecule is indicated with an asterisk. A small fraction is also broken down to heavy and light chains −50 and 25 kDa respectively. The more abundant additional bands are clearly visible in the CtPB2 IP lanes, although the scanned image does not depict less abundant proteins segregating into faintly stained bands. The horizontal lines indicate the cutting sites when slicing the gel into discrete portions for sequencing.

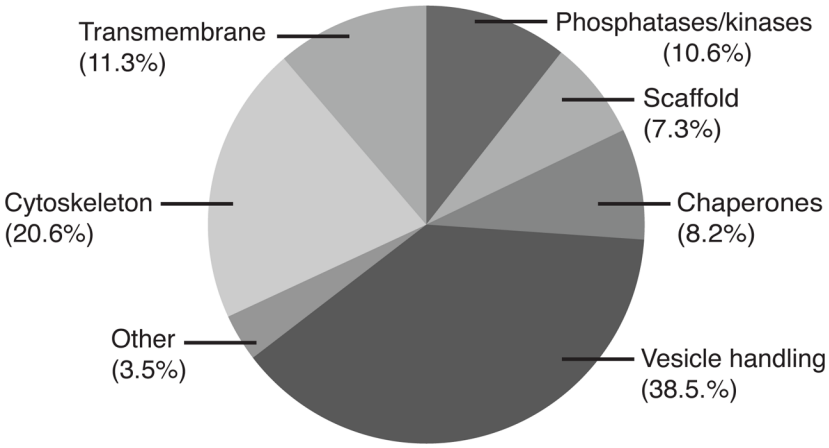

Figure 4.
Schematic representation of protein groups' molar quantities.

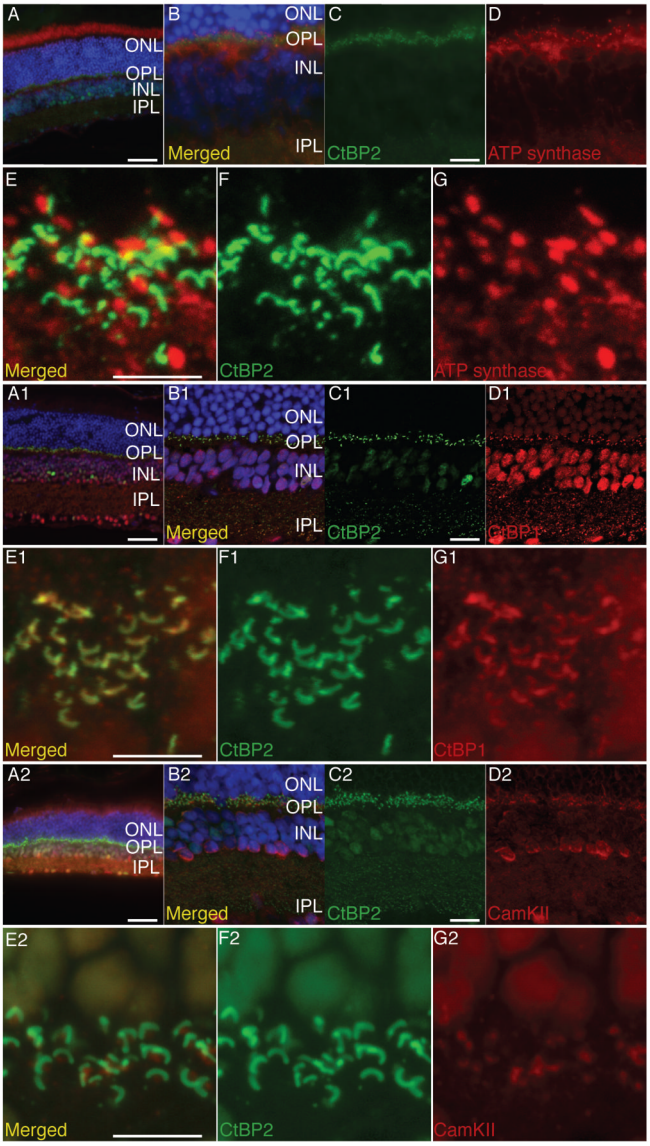

Figure 5. IHC staining for ATP Synthase, CtBP1 and CaM Kinase II in relation to CtBP2 on adult mouse retina

Panels A, A1 and A2 show an overview of the retinal staining, while panels (B, B1, B2, C, C1 and C2) show medium magnification of the inner and outer plexiform layers. Panels EG, E1-G1 and E2-G2 display high magnification the spatial relation between CtBP2 in green and ATP Synthase CtBP1 and CaM Kinase respectively in red at the outer plexiform layer. Note that even when the two proteins are not colocalized they are juxtaposed. Scale bar in A, A1 and A2 is 50 μm, scale in C, C1 and C2 in 10 μm and in E, E1 and E2 is 5 μm.

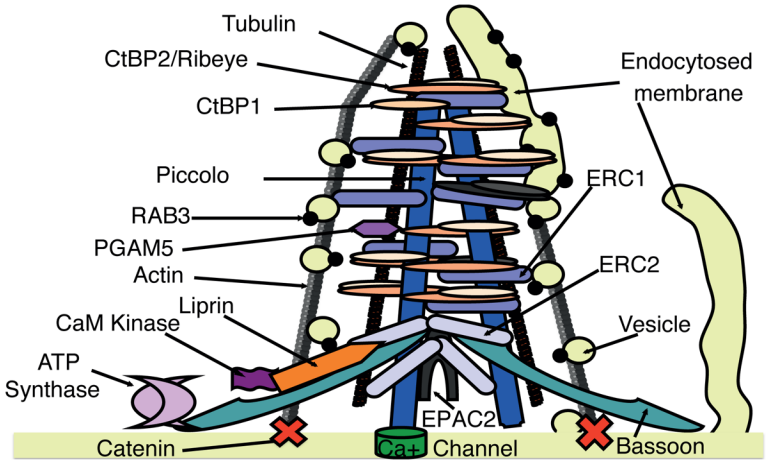

Figure 6. Synaptic ribbon composition and function. We have depicted the ribbon based in large part on known interactions and localizations of its protein constituents.<

br>Binding of Liprin and ERC1 and Erc2[16], Liprin and Cam KInase II[44], Ribeye and Bassoon[13], CtBP1 and Bassoon[13], ERC1 and Piccolo[15], ERC1 and Bassoon[15] have been described. Piccolo binds Actin-Binding Protein1, which in turn binds Actin, while actin also binds Catenin[33,48]. We have placed ATP Synthase and PGAM5 speculatively in our proposed model. The right hand portion of the figure illustrates the hypothesis that CtBP isoforms create vesicles by fission of endocytosed membranous cisterns.

J Proteome Res. Author manuscript; available in PMC 2013 February 3.

Table 1

Quantified proteins in the ribbon complex

The names the proteins, that passed our criteria, are listed in the 1st (Uniprot abbreviation) and 2nd columns. Columns 3 and 4 describe the number of unique peptides observed and observable for each protein. Those numbers were used to calculate the emPAI value given in the 5th column and derive the molar % ratio for individual proteins and protein groups of closely related isoforms and/or quaternary structures (columns 6 and 7 respectively). The 8th column shows the number of unique peptides in the IgG precipitates. Column 9 shows overlap between mouse and cow data. Most mouse proteins were also present in our bovine list of ribbon candidates as an exact match (indicated with two dots), or were represented by protein homologues (indicated with one dot), and only a few were absent in the bovine data set, which can be attributed at least partially to poor data annotation (for example Bassoon protein).

Uniprot name	Protein	Calc. uniq. pept.	Observable	emPAI	% by individ. prot.	% group proteins	# pept. in Contr.	Bovine Overlap
ACTA2	α-Actin-2	3.75	73	0.13	1.09	5.88	0	•
ACTB	Cytoplasmic Actin 1	4.75	75	0.16	1.36		2	•
ACTB	Putative Actin	5.75	74	0.2	1.7		0	•
ACTG1	γ Actin-Like Protein	5.75	73	0.2	1.73		0	••
ATP1A1	Na/K- ATPase α1	2	185	0.03	0.22	1.92	0	••
ATP1A3	Na/K- ATPase α3	3	180	0.04	0.34		1	••
ATP1B1	Na/K- ATPase α1	5	79	0.16	1.36		0	••
ATP5A1	ATP Synthase, subunit α	16	143	0.29	2.55	5.78	3	••
ATP5B	ATP Synthase, subunit β	14	102	0.37	3.23		2	••
BSN	Bassoon	8	675	0.03	0.24	1.45	0	
PCLO	Piccolo	53	933	0.14	1.21		0	••
CACNA2D4	VCa Channel α-2/δ-4	3	162	0.04	0.38	1.12	0	•
CACNB3	VCa Channel β-3	4	113	0.08	0.74		0	•
CAMK2A	CaM Kinase II α	3.5	99	0.08	0.74	2.97	0	••
CAMK2B	CaM Kinase II β	3.5	100	0.08	0.73		0	••
CAMK2D	CaM Kinase II δ	7	101	0.17	1.5		0	••
CASK	Cask	8	211	0.09	0.79	0.79	0	••
CtBP1	C-terminal Binding Protein	23.5	69	1.19	10.34	30	0	••
CtBP2	C-terminal Binding Protein	37.5	73	2.26	19.66		0	••
CTNNA2	Catenin α-2	12	234	0.13	1.09	2.07	0	••
CTNNB1	Catenin β-1	6	129	0.11	0.98		0	••

Uniprot name	Protein	Calc. uniq. pept.	Observable	emPAI	% by individ. prot.	% group proteins	# pept. in Contr.	Bovine Overlap
EML5	EML5	13	435	0.07	0.62	0.62	0	••
EPB41	Band 4.1-Protein	5.5	222	0.06	0.51	1.36	0	••
EPB41L2	Band 4.1-Like Protein 2	7.5	272	0.07	0.57		0	•
EPB41L3	Band4.1-Like Protein 3	3	220	0.03	0.28		0	••
ERC1	ELKS1/CASK2	31.5	365	0.22	1.91	6.17	0	••
ERC2	CAST1/ELKS2	56.5	326	0.49	4.26		0	••
GABRA1	GABA Rec. α 1	6	110	0.13	1.16	2.5	0	••
GABRB2	GABA Rec. 2β	2.5	99	0.06	0.52		0	••
GABRB3	GABA Receptor β3	2.5	88	0.07	0.59		0	••
GABRG2	GABA Receptor γ2	1	87	0.03	0.23		0	•
GLUL	Glutamine Synthetase	4	76	0.13	1.12	1.12	0	••
GPHN	Gephyrin	9	158	0.14	1.22	1.22	0	••
GRIP1	Glutamate Rec. Inter. Prot. 1	8	207	0.09	0.81	0.81	0	••
HSPA1B	Heat Shock 70 kDa Prot. 1	8.83	156	0.14	1.21	8.18	0	••
HSPA5	Heat Shock 70 kDa Prot. 5	13.33	157	0.22	1.88		0	••
HSPA8	Heat Shock 70 kDa Prot. 8	17.83	163	0.29	2.49		2	••
HSPA9	Heat Shock 70 kDa Prot. 9	7.5	188	0.1	0.84		0	••
HSPD1	Heat Shock Protein 60	12.5	155	0.2	1.77		0	••
MYH10	Myosin10	7	648	0.03	0.22	0.22	0	••
NEFL	Neurofilament Light	6	159	0.09	0.79	0.79	0	••
PGAM5	Ser/Thr-Phosphatase	10	82	0.32	2.82	2.82	0	
PPFIA2	Liprin-α2	7	356	0.05	0.4	0.4	0	••
PPP2R1A	Ser/Thr Phosphatase Regulatory subunit α	9	121	0.19	1.62	1.62	0	••
RAPGEF4	Rap Guanine Nucleotide Exchange Factor 4	33	245	0.36	3.16	3.16	0	••
RIMBP2	RIM-Binding Protein 2	4	180	0.05	0.46	0.46	0	
SAG	S-arrestin	5	88	0.14	1.21	1.21	1	••
SPNA2	Spectrin α	22	763	0.07	0.6	1.08	0	•
SPTBN1	Spectrin β	16	679	0.06	0.48		0	••
SRCIN1	SRC Kinase Inhibitor 1	5	340	0.03	0.3	0.3	0	••

Uniprot name	Protein	Calc. uniq. pept.	Observable	emPAI	% by individ. prot.	% group proteins	# pept. in Contr.	Bovine Overlap
TRIM21	Trim21	5	118	0.1	0.89	0.89	1	••
TUBA1B	Tubulin α-1B	7.5	63	0.32	2.74	10.94	2	••
TUBA4A	Tubulin α-4A	4.5	76	0.15	1.27		0	••
TUBB2A	Tubulin β-2A	7.17	68	0.27	2.39		2	••
TUBB2C	Tubulin β-2C	6.67	68	0.25	2.2		1	••
TUBB5	Tubulin β-5	7.17	69	0.27	2.35		2	••

Table 2
Nuclear proteins co-purified with CtBP2 Ab

The names of the nuclear proteins, which passed our threshold criteria, are listed in the 1st (Uniprot abbreviation) and 2nd columns. In the 3rd and 4th columns are shown the number of unique peptides in the CtBP2 and IgG precipitates respectively. Column 5 shows overlap between mouse and cow data. The exact matches for mouse proteins present in our bovine list of co-precipitates are indicated with two dots, while those represented by close protein homologues are indicated with one dot. Only a few proteins were absent in the bovine data set (no dots).

Uniprot name	Protein	# uniq. pept. in CtPB2 IP	# uniq. pept. in IgG IP	Bovine Overlap
AOF2	Lysine-Specific Histone Demethylase	9	0	
DDX5	RNA Helicase DDX5	8	0	••
HIST1H1C	Histone H1.2	4	0	••
HIST1H2BF	Histone H2B type	5	1	•
HNRNPM	Heterogeneous Nuclear Ribonucleoprotein M	5	0	••
LMNB1	Lamin-B1	16	1	••
MYEF2	Myelin Expression Factor 2	4	0	
PABPC1	Polyadenylate-Binding Protein 1	5	1	•
RBM14	RNA- Binding Protein 14	16	1	••
RBM9	RNA- Binding Protein 9	4	0	•
SCAI	Suppressor of Cancer cell Invasion Protein	10	0	••
C20ORF112 HOMOLOG	Similar to Nucleolar Protein 4 Isoform 1	9	0	••

Table 3
Minor co-purified proteins (including nuclear)

Cytoplasmic and nuclear proteins, that did not pass our threshold criteria, are listed in the 1st (Uniprot abbreviation) and 2nd columns. In the 3rd and 4th columns show the number of unique peptides in the CtBP2 and IgG precipitates respectively. Column 5 shows overlap between mouse and cow data. The exact matches for mouse proteins present in our bovine list of co-precipitates are indicated with two dots, while those represented by close protein homologues are indicated with one dot. Only a few proteins were absent in the bovine data set (no dots).

Uniprot name	Protein	# uniq. pept. in CtPB2 IP	# uniq. pept. in IgG IP	Bovine Overlap
ACAD9	Acyl-CoA Dehydrogenase Family Member 9	2	0	•
CLTC	Clathrin Heavy Chain 1	2	0	••
DPYSL2	Dihydropyrimidinase-Related Protein 2	3	0	••
GNB1	Guanine Nucleotide-Binding Protein Subunit β-1	2	0	••
HTRA1	Serine Protease HTRA1	3	0	
IMMT	Mitochondrial Inner Membrane Protein	2	0	••
INA	Alpha-Internexin	2	0	••
MYO6	Myosin-VI	2	0	••
NLGN2	Neuroligin-2	2	0	••
NSF	Vesicle-Fusing ATPase	2	0	••
RPH3A	Rabphilin-3A	3	0	••
RPLP0	60S Acidic Ribosomal Protein P0	2	0	••
RPSA	40S Ribosomal Protein SA	2	0	•
SYN1	Synapsin-1	3	0	••
SYN2	Synapsin-2	2	0	•
SYNGR3	Synaptogyrin-3	2	0	••
SYT1	Synaptotagmin-1	2	0	••
TRAPPC9	Trafficking Protein Particle Complex subunit 9	2	0	
	— NUCLEAR PROTEINS —			
DDX17	Probable ATP-dependent RNA Helicase DDX17	2	0	•
EIF4A3	Eukaryotic Initiation Factor 4A-III	3	0	
FMR1	Fragile X Mental Retardation Protein 1 homolog	2	0	•
HDAC2	Histone Deacetylase 2	2	0	
PURB	Transcriptional Activator Protein Pur- β	3	0	•
ZNF516	Zinc Finger Protein 516	2	0	